International Journal of Energetica (IJECA)
https://www.ijeca.info
ISSN: 2543-3717 Volume 6. Issue 1. 2021
Page 43-54

Numerical study of a hybrid photovoltaic/thermal PVT solar collector using three different fluids

A. Ghellab[*1,2], T.E. Boukelia[*2,3], S. Djimli[1,2], A. Kaabi[4]

[1]*Laboratory of Applied Energies and Materials, Faculty of Sciences and the Technology, Ouled Aissa BP 98, University of Jijel, ALGERIA*
[2]*Mechanical Engineering Department, Faculty of Sciences and the Technology, Ouled Aissa BP 98, University of Jijel, ALGERIA*
[3]*Laboratory of Mechanical and Advanced Materials, Polytechnic School of Constantine, Constantine, ALGERIA*
[4]*Climatic Engineering Department, Faculty of Science and Technologies, Route Ain El Bey, University of Constantine1, ALGERIA*

*.Email *:ghellab_amel@yahoo.fr and taqy25000@hotmail.com*

Abstract – *Hybrid photovoltaic and thermal (PV/T) systems have been widely used for the combination of PV modules and solar thermal collectors to generate both electrical energy and heat at the same time. In the present work, a numerical model has been developed to simulate the performances of a hybrid photovoltaic/thermal (PV/T) solar collector. Furthermore, a comparative study has been performed between the hybrid PV/T working with three conventional working fluids; air, water, and specified nanofluid (AL2O3+ water). The obtained results show that the use of the Alumina nanofluid is the best choice to increase the heat removal, and to improve the performances of the collector with the values of 73.28%, 10.37% and 99.21% for the thermal, electrical and global efficiency respectively. On the other hand, the PVT collector working with air as the primary fluid is the worst in terms of electrical, thermal, and global performances with the lowest values of 9.506 %, 41.55%, and 65.315% respectively.*

Keywords: *Hybrid solar collector, Nanofluid, Numerical study, Performance, Nanofluid.*
Received: 30/03/2021 – Accepted: 29/06/2021

I. Introduction

Many academics from all over the world are attempting to meet the rising need for energy, by developing different types of solar collectors to provide a clean energy in sufficient quantities and at low costs. For many decades, the hybrid photovoltaic and thermal (PV/T) systems have been widely used for the combination of PV and solar thermal effects to generate both electrical and thermal energies, as it is well-known that the cell efficiency is decreasing with high temperatures. Theoretical and also experimental research on hybrid PV/T systems using air and/or water as working fluids were documented. For example, Previous research [1-2] found that the flat plate photovoltaic thermal (PV/T) solar collector is a good option for low-energy applications in homes, commercial buildings, and industrial. Prakash [3] has presented a dynamic model of a hybrid PV/T solar systemusing two fluids; air and water as working fluids. It was reported that the thermal efficiency varies from 50% to 67% for water heating, and from 17% to 51% for air heating. In the case of air heating, the lower thermal efficiency is attributable to the poor conductivity and specific heat of air compared to water. A study has developed an analytical mode to compare and contrast the performance of a PV/T collector with two layouts; single and double pass. They concluded that the double pass PV/T collector outperformed the single pass PV/T collector [4]. However, another study has showed a PV/T air heater with four designs for single and double pass. He developed the thermal model of every system, then examined the effect of air specific flow rate on the performance of each one [5]. Nine distinct designs of a combination PV/T water/air solar collector were evaluated by a research group, they revealed that the best design is the sheet-and-tube collector with single cover

[6]. An explicit dynamic model has been performed a PV/T collector with a single glazed flat plate for water heating. The model captured the instantaneous energy outputs and allowed for a detailed investigation of transient behavior across multiple collector components [7]. A theoretical model was developed to study the effect of the channel dimension, as well as the mass flow rate on the performance of such system. The results were validated with those issued by their experience [8]. The paper looked at hybrid PV/T systems that extract heat from PV modules using air or water. He also experimented with three different ways to place the water heat exchanger inside the air channel; the modified twin PV/T collectors were combined with booster diffuse reflectors to improve the PV/T systems' electrical and thermal output. By integrating low-cost extra system elements, the recommended combination of diffuse reflectors improved the effective operation on horizontal building roof installation [9]. Scientific work has focused on an experimental study by adding the propylene glycol (PG) in water as a working fluid in a PV/T solar collector. Their obtained results indicated that the using of PG-water at 25% PG concentration, reduced the efficiency of the flat plate solar collector by 15.68%, compared with pure water [10]. A hybrid PV/T collector with water as working fluid produced in a copolymer material was also described and simulated in another study. They pointed out that using the copolymer reduces the weight and cost of such systems, as well as making them easier to manufacture [11]. Investigation has studied the performances of a PV/T air heater with a double pass layout, and vertical fins in the bottoming channel of the absorber surface. Such enhancement improves the heat transfer area to air, and increases the efficiencies of this form of collector, according to the researchers [12].

The literature showed the enormous efforts which have been made to enhance the heat extraction from the cells in a solar PV/T collector, in order to improve the electrical conversion efficiency by using cooling fluids which have higher thermo-physical proprieties. This condition can be realized by adding ultra-fine solid particles of millimeter or micrometer size to the working fluid. On this direction, most of research works were mainly based on nanofluids, which are composed of particles dispersed in water with various concentrations ranging. Based on previous research's review papers [13-15], In solar thermal systems, nanofluids can be used to improve the thermal efficiency and performance of the solar collector. They found that producing a nanofluid-based solar collector emits roughly 170 kg/year less CO_2 on average than a traditional solar collector, implying that nanofluid causes less environmental damage. However, the reviews [16-18] summarized the recent correlations developed to analyze the free and forced heat transfer convection phenomena in flow with nanofluids. A group of scientists has proposed a new correlation for the convective heat transfer of a Cu-water nanofluid for both laminar and turbulent flow conditions. They determined that this correlation takes into consideration the major elements impacting nanofluid heat transfer and that the presence of nanoparticles improves heat transfer performance [19]. On the other hand, another group has performed a comprehensive analysis in order to evaluate the effects of variations in volume fraction and temperature of nanofluid on its density, specific heat, thermal conductivity and viscosity [20]. The effect of cooper nanoparticles in the presence of a magnetic field on unsteady non-Darcy flow and heat transfer over a porous wedge due to solar radiation has been studied theoretically [21]. Another research has studied numerically the heat transfer and pressure drop of three different nanofluids which were: copper oxide (CuO), alumina (Al2O3), oxide titanium (TiO2), and water as based fluid. The results illustrated that by increasing the volume of concentration of nanoparticles, the heat transfer coefficient increased. Furthermore, for a constant volume of concentration, the effect of CuO nanoparticles to enhance the Nusselt number was better than the two other nanoparticles; Al2O3 and TiO2 [22]. Study have reported the results of an experiment analysis, and have studied the effect of Al2O3-H2O nanofluid as an absorbing medium on the efficiency of flat plate solar collector. The results of the experiment showed that the use of a concentration of 0.2 % Al2O3 nanofluid increased the efficiency of the solar collector in comparison with water as working fluid by 28.3%, and by using surfactant the maximum enhanced efficiency is about 15.63% [23]. Scientific analysis has analyzed the effect of nanofluid on the performances of an absorber of a direct solar collector. They showed that the particle size has minimal influence on the optical proprieties of nanofluid, and the extinction coefficient is linearly proportionate to volume fraction [24]. Another scientific analysis has studied experimentally the forced convection flow of aluminum oxide nanoparticles dispersed in water through a circular pipe. The results showed that the presence of nanoparticles in the working fluid caused a remarkable increase in the heat transfer comparing to the working fluid itself [25]. Furthermore, scientific team have investigated experimentally the effect of density, thermal conductivity and viscosity of water and Ethylene glycol water mixture (60:40 by mass) based alumina nanofluids, on the pressure drop and pumping power for

a flat plate solar collector. It was observed that the viscosity of the Al2O3-water nanofluids exponentially decreased with increasing in working temperature, and they have indicated the non-linear relation between viscosity and concentration. They showed that the pressure drops and consumed power for fluid pumping of nanofluid flows are almost similar to that of the base liquid with low concentration [26]. Another team have performed a numerical simulation of the heat transfer enhancement and behaviors of water-γ Al2O3, and Ethylene Glycol- γ Al2O3 nanofluids in two different confined flow situations. Their findings revealed that the use of nanoparticles resulted in a significant increase in heat transmission. However, and according to our knowledge concluded from literature, no comparative study has been presented to compare the performances of these systems using different working fluids, thus, the objective of the present study is to use nanoparticles within the working fluid for a hybrid PV/T solar collector, and to make a comparison in terms of efficiencies between this solar collector with three different fluids (air, water, and Alumina nanofluid (Al2O3+water)) [27].

This study takes Constantine (North-east of Algeria) as a case study, and a numerical model is developed by presenting energy balances for different nodes: glazing, PV cell, absorber, fluid and back plate, and considering the transient effects.

II. Description of the studied PV/T collector

Figure 1 shows a cross-sectional view of the proposed photovoltaic/thermal (PV/T) collector. The investigated system is made up of transparent glazing located at the top of the collector, which transmitted the incident solar radiation to the solar cell, and the absorber at the bottom of PV/T collector. The stagnant air in the air gap is assumed circulate under free convection. A fraction of the incident radiation is converted into electricity by the solar cell, and into heat by the absorber, which transfer the heat to the fluid flowing into a rectangular duct formed by the top absorber, and the back metallic plate supposed painted black. The cooling fluid is flowing under forced circulation mode. The conduct bottom is insulated in order to minimize heat losses with the ambient. The inclination angle of the studied hybrid V/T solar collector is taken equal to the latitude of Constantine east town in Algeria.

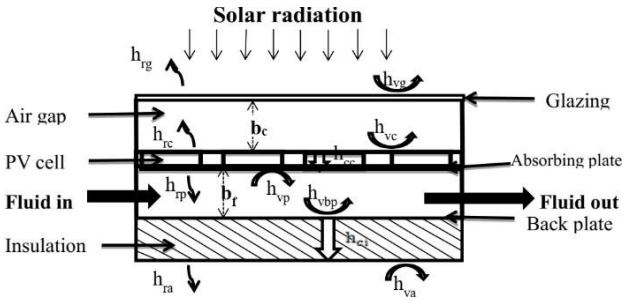

Figure 1. A cross sectional view of the studied hybrid PV/T solar collector

III. Mathematical modelling

To examine the PV/T performances, a transient mathematical model under forced convection was constructed. In order to write the energy balance between the components, it would be convenient to use the analogy between electricity and heat transfer. Fig.1 shows the different heat transfer coefficients along various elements of the collector. It is necessary to make some assumptions to model the system considered, as:

- ✓ The sky can be compared to a black body with equivalent calculated temperature.
- ✓ The temperature of the soil is taken equal to the ambient temperature.
- ✓ The physical proprieties of materials are assumed to be constant.
- ✓ The wind is supposed blowing parallel to the faces of the system.
- ✓ The fluid entering the duct is at room temperature, and the ducts fluid temperature is a combination of the input and exit temperatures.

The following are the energy balance equations for different surfaces of the PV/T collector:

- Glazing:

$$m_g c_g \left(dT_g/dt\right) = P_g A_g + h_{vg}(T_a - T_g)A_g + h_{rg}(T_s - T_g)A_g + (h_{vc} + h_{rc})(T_c - T_g)A_g \quad (1)$$

Where m_g, c_g and A_g denote the mass, specific heat and area of glass respectively, while P_g represents the rate of the energy absorbed by the glass, $h_{vg}$and h_{rg} are the heat transfer coefficients based on convection and radiation between the glazing and ambiance/sky respectively. On the other hand, $h_{vc}$is the convection heat transfer coefficient for air cavity between the solar cell and glazing, h_{rc} is the heat transfer coefficient based on radiation between solar cell and glazing. T_g,T_a T_s and T_c represent respectively temperatures of: glass, ambient, sky and PV cell and t represents the time. The

quantity of the energy absorbed by the glass is calculated by the following expression [28]:

$$P_g = P_{dir} \cdot \alpha_{g-dir} + P_{dif} \cdot \alpha_{g-dif} \quad (2)$$

Such as P_{dir} and P_{dif} represents respectively the intensity of the direct and diffuse incident radiation. The absorption coefficients of glazing α_{V1-dir} et α_{V1-dif} are calculated from [28].

The coefficient of radiation heat transfer from the glazing to the sky is given by [29]:

$$h_{rg} = \sigma s_g (T_g^4 - T_s^4) / (T_g - T_a) \quad (3)$$

Where σ is the stephan-Boltzmann constant, s_g is the emissivity of thermal radiation of the glass cover, T_g characterize the sky temperature which is evaluated by Swinbank (1963) as follows [29]:

$$T_s = 0.0552(T_a)^{1.5} \quad (4)$$

The coefficient of convective heat transfer between the glazing and ambiance is formulated by Mc Adams (1954) [29]:

$$h_{vg} = 5.7 + 3.8.v \quad (5)$$

Where v represents the wind velocity.

The coefficient of radiation heat transfer between solar cell and glazing can be calculated from the following equation:

$$h_{rc} = \sigma(T_c + T_g)(T_c^2 + T_g^2) / (1/s_c + 1/s_g - 1) \quad (6)$$

Note that the symbol s_c represents the emissivity of the solar cell.

The coefficient of convection heat transfer for air cavity between the solar cell and glazing, is given by :

$$h_{vc} = Nu.k_{air} / D_h \quad (7)$$

Where Nu represents the Nusselt number, K_{air} is the air conductivity and D_h represents the hydraulic diameter of the air flowing in the channel. The Nusselt number can be calculated by the convection between inclined parallel flat plates [29]:

$$Nu = 1 + 1.446 \left[1 - 1708 / (R_a \cos\theta)\right]^{+} \left[1 - 1708[\sin(1.8)]^{1.6} / (R_a \cos\theta)\right] + \left[(R_a \cos\theta / 5830)^{0.333} - 1\right] \quad (8)$$

Where R_a represents the Rayleigh number and θ is the collector inclination angle, which can be calculated by the following expression:

$$Ra = \rho^2 c_p g \beta (T_c - T_g) b^3 / k_{air} \mu \quad (9)$$

Where ρ, c_p, β and μ are respectively the density, specific heat, thermal expansion coefficient and the dynamic viscosity of air, and g is the gravitational constant.

- Solar cell:

$$m_c c_c (dT_c/dt) = P_c . A_c + (h_{vc} + h_{rc})(T_g - T_c)A_c + h_{cc}(T_p - T_c)A_c - Q_{ele} . A_c \quad (10)$$

Where m_c, c_c and A_c represents respectively the mass, specific heat and area of the solar cell, P_c represents the rate of the energy absorbed by the PV cell, h_{cc} is the heat transfer coefficient conduction between the PV cell and the absorber plate and Q_{ele} is the electrical power produced by the PV module. T_c Represents the PV cell temperature and T_p represents the absorbing plate temperature. The rate of solar energy received by solar cell after transmission is calculated by the following expression [30]:

$$P_c = r_g \times \alpha_c \times \beta_c \times P_g \quad (11)$$

Where α_c is the absorption coefficient of the cell and β_c is the Packing factor which represent the ratio of cell area to aperture area. While the rate of electrical energy generated by the PV cell can be calculated by [30]:

$$Q_{ele} = 5_{ele} \times P_g \times \beta_c \times r_g \quad (12)$$

Where 5_{ele} design the electrical efficiency generated by the cell, which is estimated by the relation (38) and r_g is the transmission coefficient of the glass. The heat transfer coefficient conduction between the PV cell and the absorber is calculated by:

$$h_{cc} = {}^{k_c}/_{e_c} + {}^{k_p}/_{e_p} \quad (13)$$

k_c, k_p and e_c, e_p are respectively the thermal conductivity and the thickness of PV cell and absorbing plate.

- Absorbing plate:

$$m_p\, c_p\, ({}^{dT_p}/_{dt}) = h_{cc}(T_c - T_p)A_c + h_{vp}(T_f - T_p)A_p + h_{rp}(T_{bp} - T_p)A_p + A_p P_p \quad (14)$$

Where m_p, c_p and A_p represents respectively the mass, specific heat and area of the absorber plate, P_p represents the rate of the energy absorbed by the absorbing plate, h_{vp} is the heat transfer coefficient convection between the absorber plate and the fluid, $h_{rp}$is the heat transfer coefficient by radiation between the absorber and back plate. T_f and T_{bp} represent the temperatures of fluid and back plate respectively. P_p is the rate of solar energy absorbed by the absorbing plate, which is calculated by:

$$P_p = r_g \times (1 - \beta_c) \times \alpha_c \times P_g \quad (15)$$

The heat transfer coefficient by radiation between the absorber and back plate can be given as [29]:

$$h_{rp} = \sigma(T_p + T_{bp})(T_p^2 + T_{bp}^2) \,/\, ({}^1/_{s_{bp}} + {}^1/_{s_p} - 1) \quad (16)$$

Where s_{bp} And s_p are respectively the back plate and the absorber coefficients of emissivity.

- Fluid flowing in the duct:

$$m_f\, c_f\, ({}^{dT_f}/_{dt}) = h_{vp}(T_p - T_f)A_f + h_{vbp}(T_{bp} - T_f)\, A_f - \dot{m}\, c_f(T_{out} - T_{in})A_f \quad (17)$$

Where m_f, c_f and A_f represents the mass, specific heat and area of the fluid respectively, h_{vbp} is the heat transfer coefficient convection between the fluid and the back plate, T_{in} and T_{out} represent respectively the inlet and the outlet temperatures of the fluid in the duct, $\dot{m}$ is the mass flow rate of the primary cooling fluid.

- Back plate:

$$m_{bp}c_{bp}\, ({}^{dT_{bp}}/_{dt}) = h_{vbp}(T_f - T_{bp})A_{bp} + (h_{ci} + h_{va})(T_a - T_{bp})A_{bp} + h_{rp}(T_p - T_{bp})A_{bp} + A_{bp}h_{ra}(T_{soil} - T_{bp}) \quad (18)$$

Where m_{bp}, c_{bp} and A_{bp} represents respectively the mass, specific heat and area of the back plate, h_{ci} is the heat transfer conduction coefficient in the insulation, h_{ra} is the radiation heat transfer coefficient from the back plate and soil, h_{va} is the convective heat transfer coefficient for air cavity between the back plate and soil. T_{soil} represents the temperature of the soil. The heat transfer coefficient by conduction in the insulation can be obtained by:

$$h_{ci} = {}^{k_i}/_{e_i} + {}^{k_{bp}}/_{e_{bp}} \quad (19)$$

With k_i, k_{bp} and e_i, e_{bp} are respectively the insulating and back plate thermal conductivity and thickness.

The radiation heat coefficient between back plate and soil is calculated by:

$$h_{ra} = \sigma s_{bp}(T_{soil} + T_{bp})(T_{soil}^2 + T_{bp}^2) \quad (20)$$

The convective heat coefficient between back plate and soil H_{va} can be taken the same as H_{vg}.

III.1. Expression of convective heat transfer coefficients

For convective exchange between two metallic plates and the fluid inside the duct, the heat transfer coefficient can be calculated by:

$$h_{vp} = h_{vi} = Nu\, {}^{k_f}/_{D_h} \quad (21)$$

Where k_f is the fluid thermal conductivity, Nu is the Nusselt number for forced convection in the duct formed by the absorbed plate and the back plate. According to the literature analysis, this number can be expressed for different fluid examined in this work as:

- For air:

According to [29] and [31], the correlation of Tan and Charters (1970) is recommended for parallel flat plate and Nusselt number can be expressed by:

$$Nu_{air} = 0.018\, Re_{air}^{0.8}\, Pr_{air}^{0.4} \quad (22)$$

Where Pr_{air} is the Prandtl number of air, Re_{air} is the Reynolds number of air defined as:

$$Re_{air} = \rho^{v} . D_h / \mu \quad (23)$$

In which ρ and μ represent the density and the dynamic viscosity of air, v is the mean velocity of air in the duct.

- For water:

Referring to [32], the Nusselt number of pure water for turbulent flow in two parallel plates, can be calculated by the following correlation over the well-known equation of Dittus-Boelter:

$$Nu_{water} = 0.023\ Re_{water}^{0.8}\ Pr_{water}^{0.33} \quad (24)$$

Where Pr_{water} is the Prandtl number of water, Re_{water} is the Reynolds number of water.

- For nanofluid:

According to [27, 33], the following correlation has been created to determine the Nusselt number in terms of Reynolds and Prandtl numbers [16], of turbulent flow in tube using Al_2O_3 – water mixture under a uniform heat flux boundary condition on its wall.

$$Nu_{nf} = 0.085\ Re_{nf}^{0.71}\ Pr_{nf}^{0.35} \quad (25)$$

For $6.6 \leq Pr_{nf} \leq 13.9$, $10^4 \leq Re_{nf} \leq 5.10^5$ and $0 < \varphi < 10\ \%$

Where Pr_{nf} , Re_{nf} represent the Prandtl and the Reynolds number of the nanofluid and φ represents the volume fraction of Al_2O_3 nanoparticles.

III.2. Expression of thermo-physical properties

- For air:

According to [29], the physical properties of air are assumed varying with temperature, as follows:

✓ Viscosity

$$\mu_{air} = [1.983 + 0.00184(T_f - 27)]10^{-5} \quad (26)$$

✓ Density

$$\rho_{air} = 1.1774 - 0.00359(T_f - 27) \quad (27)$$

✓ Thermal conductivity

$$k_{air} = 0.02624 + 0.0000758(T_f - 27) \quad (28)$$

✓ Specific heat

$$c_{p,air} = 1.0057 + 0.000066(T_f - 27) \quad (29)$$

- For water:

The equations of the physical proprieties of water are obtained from the equations provided in the study by Jayakumar et al [34], as:

✓ Viscosity

$$\mu_{water} = 2.1897\ \exp(-11)\ T_f^4 - 3.055\ \exp(-8)\ T_f^3 + 1.6028\ \exp(-5)\ T_f^2) - 0.0037524\ T_f + 0.33158 \quad (30)$$

✓ Density

$$\rho_{water} = -1.5629\ \exp(-5)\ T_f^3 + 0.011778\ T_f^2 - 3.0726\ T_f + 1227.8 \quad (31)$$

✓ Thermal conductivity

$$k_{water} = 1.5362\ \exp(-8)\ T_f^3 - 2.261\ \exp(-5)\ T_f^2 + 0.010879\ T_f - 1.0294 \quad (32)$$

✓ Specific heat

$$c_{p,water} = 1.1105\ \exp(-5)\ T_f^3 - 0.00310\ T_f^2 - 1.478\ T_f + 4631.9 \quad (33)$$

- For nanofluid:

From literature, the physical proprieties of nanofluids depend on parameters including the thermal proprieties of the water as base fluid and the volume fraction of aluminum oxides (Al_2O_3) nanoparticles dispersed in water. Based on the report [27], the Eqs (34) and (35) are general relationships used to compute specific heat and the density for a classical two-phase mixture. The specific heat of the Al_2O_3-water nanofluid can be calculated by [27]:

$$c_{p,nf} = (1 - \varphi)c_{p,water} + \varphi c_{p,np} \quad (34)$$

Where $C_{p,nf}$, $C_{p,water}$ and $C_{p,np}$ represent respectively the specific heat of nanofluid, base fluid and nanoparticle. The nanofluid density is calculated by the following relation [27]:

$$\rho_{nf} = (1 - \varphi)\rho_{water} + \varphi\rho_{np} \quad (35)$$

Where ρ_{nf}, ρ_{water} and ρ_{np} represent respectively the density of nanofluid, base fluid and nanoparticle.

They exist several semi-empirical correlations for calculating thermal conductivity and the dynamic viscosity. Recent models have shown that numerical simulations for viscosity and thermal conductivity require more robust models that account for temperature dependency and nanoparticle size. These correlations include temperature and volume fraction [26, 35] in the eq (36) which represents the modified statement of Nguen:

$$\mu_{np} = exp(3.003 - 0.04203T_f - 0.5445\varphi + 0.0002553T_f^2 - 0.0534\varphi^2 - 1.622\varphi^{-1} \quad (36)$$

Regarding the nanofluid thermal conductivity, and according to Maiga[27], this parameter can be calculated using the eq (37), this model has been used in this study because of his simplicity:

$$k_{nf}/k_{water} = 4.97\varphi^2 + 2072\varphi \quad (37)$$

k_{nf}, k_{water} represents respectively the thermal conductivity of nanofluid, base fluid.

III.3. Expression of efficiencies

The expression of the electrical efficiency generated by the cell is:

$$5_{ele} = 5_{ref}[1 - \beta_r(T_c - T_r)] \quad (38)$$

Where 5_{ref} is the reference cell efficiency at operating temperature T_r of 25 °C, and β_r is the coefficient of temperature and these parameters are given by manufacturer [30].

The instantaneous PV/T collector thermal efficiency of can be expressed by the heat ratio quantity extracted by the fluid used to the amount of solar radiation incident on the glazing [28]:

$$\eta_{th} = \int \dot{m}\, c_f(T_{out} - T_{in})dt / A \int P_g dt \quad (39)$$

And the overall efficiency of the PV/T solar collector is computed by adding the thermal efficiency equivalent of electrical efficiency and the thermal efficiency [30]:

$$5_{overall} = (5_{ele}/c_f) + 5_{th} \quad (40)$$

Where c_f is the conversion factor of the thermal power plant, its value can be taken as 0.4 [30].

IV. Method of resolution

Based on the finite difference formulation, the temperature distribution can be determined by a system of linear algebraic equations, these systems can be written as a matrix equation as follows [31]:

$$A(5, 5) \times T(5) = B(5) \quad (41)$$

Where A (dimension: 5) represents a square matrix, such its elements join the known thermal capacities of materials with the different heat exchange coefficients between PV/T collector elements, T *(5)* is a vector containing system of the unknown's temperatures at the nodes and the vector B *(5)* which join the constants, thermal capacities of materials with the heat exchange coefficients which related with the input physical parameters. This equation system is solved by the iterative Guass-Siedel method, which allowed evaluating the unknowns for each time and for each component. For numerical calculation, a computer program was prepared in Matlab language. First, initial guessed temperatures are used equal to ambient temperature in order to calculate the heat transfer coefficient, which can be used to estimate (T_g, T_c, T_p, T_f and T_{bp}), then the values obtained are reinserted to calculate new temperatures of various elements. If all new values are larger than 0.01% from their guessed temperature, the process is repeated until the solution converges.

V. Results and discussion

V.1. Validation results

- Air as working fluid

The values of the thermo-physical parameters for various surfaces of the system which have been used to validate the model are found from literature [5], [11], and [36]. The relevant parameters used for numerical calculations are listed in Table 1. The electrical efficiency is calculated by eq. (38), and the following values were experimentally validated according to [5]: βr=0.004 K^{-1}, η_{ref}=12.5%. Both the absorber plate and the back plate are in cooper and the values of emissivity and thickness of the back plate are taken as: ε_{bp}=0.9 and e_{bp}= 3mm [5].

Table 1. Main parameters used in simulation [5, 11 and 36].

Parameters	Glazing	PV cells	Absorbing plate	Insulation
Absorption coefficient (-)	α_g=0.04	α_c=0.9	α_p=0.94	-
Transmission coefficient (-)	τ_g=0.9	-	-	-
Emissivity (-)	ε_g=0.86	ε_c=0.7	ε_p=0.95	-
Thickness (mm)	e_g= 3	e_c= 0.22	e_p= 3	e_i=50
Thermal conductivity ($w.m^{-1}.K^{-1}$)	k_g= 1.8	k_c= 130	k_p= 386	k_i= 0.045
Density($kg.m^{-3}$)	ρ_g= 2700	ρ_c= 2330	ρ_p= 8954	-
Specific heat capacity ($J.kg^{-1}.K^{-1}$)	c_g=750	c_c=836	c_p=0.383	-

First, the program was operated on a panel with area of 9 m^2 the input data collected of the PV/T air collector Model II from the comparative study [5], in his study this model represented the highest thermal efficiency values.

Figure 2 illustrates the comparison of the thermal efficiency of the present numerical code with the thermal efficiency available in the study [5], the figure represents the variation of performances as a function of the air mass flow rate which spanning the range of 0.005-0.04 kg/s.m^2. The results obtained are in good agreement with those reported by [5]. The results of the present study predict the thermal efficiency within a relative error of $\pm 2\%$ which may come from making hypotheses and uncertainties in the correlations used in the mathematical analysis.

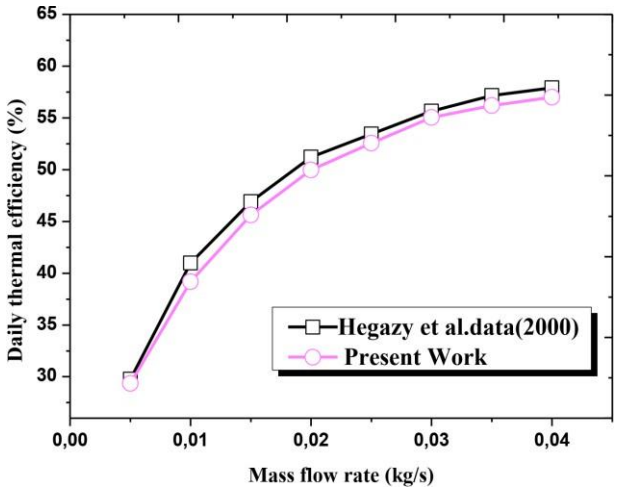

Figure 2. Comparison between the present work and those of Hegazy

V.2. *Evolution of solar radiation intensity and ambient temperature*

The following performance evaluation have been carried out for meteorological data which concern Constantine town in east Algeria (36°70', 6°37'), for the typical summer day 30 July 2015, and during which the prevailing maximal and minimal temperatures are respectively equal to 43°C and 22°C, according to [37]. The calculation of the different parameters is during the sunshine and the collector represents an area of 1m long by 1 m wide and the wind speed was taken equal to 0.5m/s. Figure 3 represents the variation of solar radiation and ambient temperature of the typical day on hourly basis. It can be seen that the radiation varies from a minimum value of 290.206 W/m^2 at 8:00h and 17:00h to a maximum value of 920.88 W/m^2 at 13:00h.

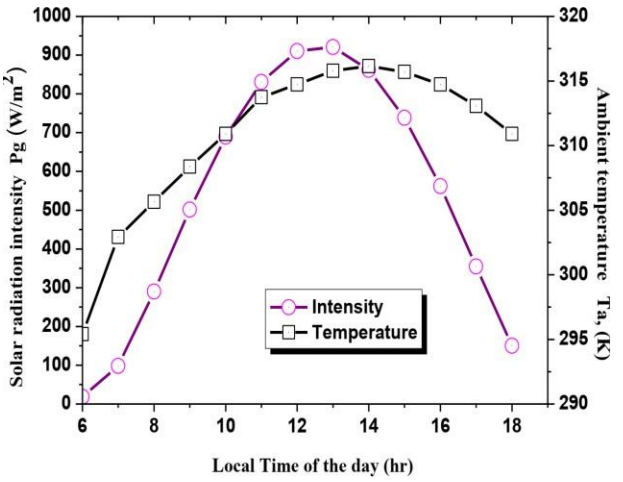

Figure 3. Hourly variation of solar intensity and ambient temperature of the typical day

V.3. *Comparative results*

The proprieties of the conventional working fluid, are evaluated as a function of temperature by using equations: Eqs (26)-(29) for air and Eqs (30)-(33) for water. However, the proprieties of the Alumina nanofluid are simulated by using Eqs (34)-(37) at different temperatures using 2% as a volume fraction of Al_2O_3 nanoparticles in the base fluid that is water.

Figure 4 shows the effect of mass flow rate on the thermal efficiency of the PV/T system. It is observed that the thermal efficiency increases with the increase of the mass flow rate and the results illustrates that the thermal efficiency of nanofluid is the highest comparing with those of water and air, since the increase in the mass flow rate, enhance the convection heat transfer from the absorbing plate to the flowing fluid and leads to reduce the thermal losses from the absorbing plate to ambiance. These results are agrees well with [5], [15] and [23].

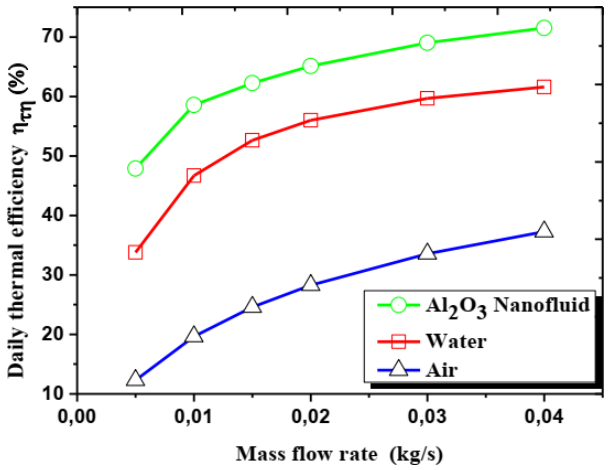

Figure 4. Variation of thermal efficiency with mass flow rate for: air, water and Alumina nanofluid

Figure 5 shows the hourly variation of the outlet temperature of three different working fluids, which were: air, water and Alumina nanofluid. The outlet temperature of different fluids increases with local time as radiation increases and present their maximum at 13:00h, because the solar radiation is collected on the absorbing plate then transferred to the working fluid and it can be seen that the outlet temperature of the Alumina nanofluid presents the highest temperature with a significant difference compared with those of water and air. Whereas, the maximum outlet temperature of nanofluid is 3.72°C higher than water and 11.77°C more than air.

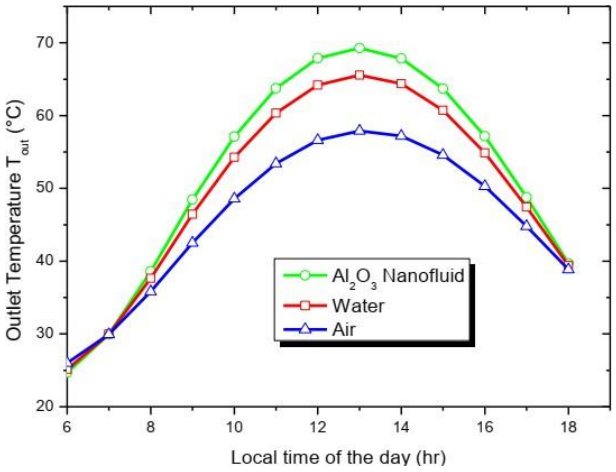

Figure 5. Comparison between the simulated outlet temperatures of different working fluids: air, water and Alumina nanofluid

Figure 6 represents the variation with time of the rate of heat extracted by the fluid when the mass flow rate is taken equal to 0.04kg/s. The results of this figure indicate that the quantity of heat extracted by the nanofluid is higher than the other two fluids, because the presence of Al_2 O_3 nanoparticles in the nanofluid enhances its thermal conductivity and density than water and air, which improves the heat transfer coefficient from the absorber plate to the flowing fluid. These results are in good agreement with that reported in literature. Values of the heat extracted by working fluid is substituted in Eq (39) to calculate the thermal efficiency which is function of the specific heat and mass flow rates of the three working fluids, because of the highest values of the outlet temperature of nanofluid, it's remarkable in Figure 7 that the thermal efficiency of the nanofluid becomes higher compared to other two fluids. The maximum values of thermal efficiency are found to be: 73.28%, 67.67% and 41.55%, of nanofluid, water and air, respectively. It's remarkable in Figure 8 that the temperature of the cell when the nanofluid is flowing is relatively lower than those of other fluids, this has a direct impact on the electrical efficiency, so it is clear in

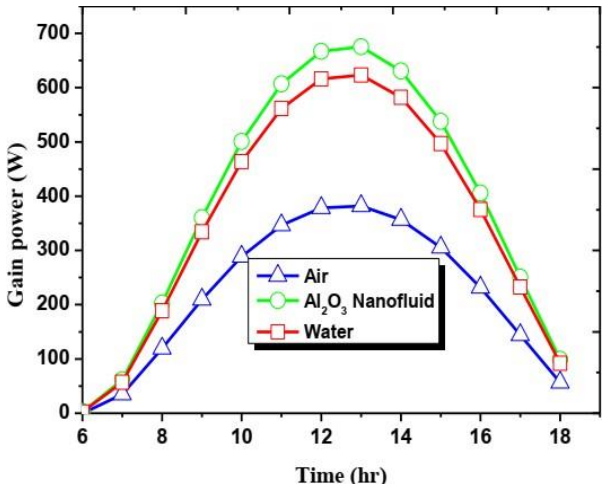

Figure 6. Hourly variation of heat gain of three fluids: air, water and Alumina nanofluid

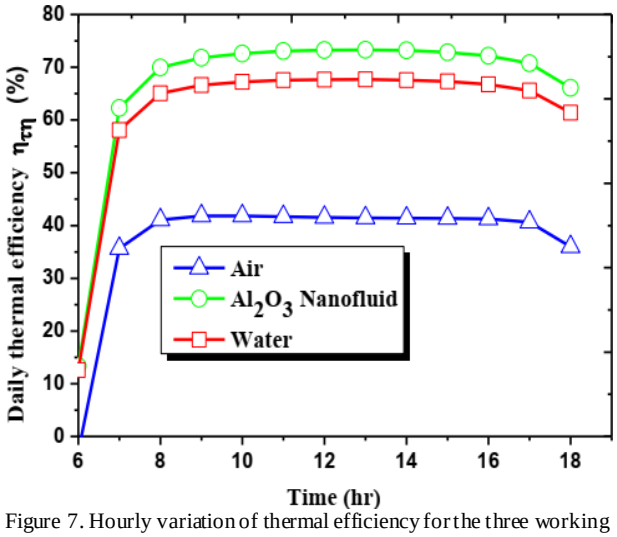

Figure 7. Hourly variation of thermal efficiency for the three working fluids

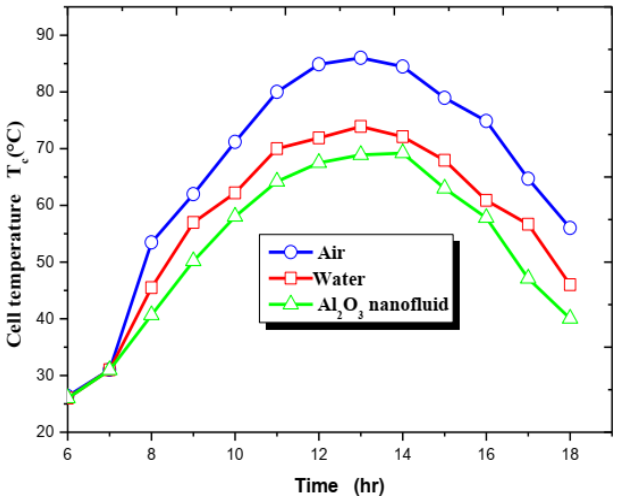

Figure 8. Hourly variation of PV cell temperature for the three cooling fluids

Figure 9 that this fluid represents the best electrical efficiency comparing to those of water and air because the increase in temperature of the cell causes the decrease in electrical efficiency. It is noted from results of Figure 7 and Figure 9 that the thermal efficiency rises when operating temperature increases but in the same time the electrical efficiency decreases, this conflict impose to calculate the overall efficiency using Eq (40) in order to determine which fluids represents the best performances of the PV/T system, the same comment was established by [5], [8] and [30], so the Figure 10 exhibits the evolution of the overall efficiency of the panel for the three fluids and it can be seen from results that the overall efficiency of Alumina nanofluids is higher by about 6.15 % and 33.9 % than water and air, respectively, because nanoparticles give the nanofluids the highest density and lower specific heat and according to [15] less heat is required to raise the temperature of the nanofluid and thus making the output temperature and efficiency becomes higher.

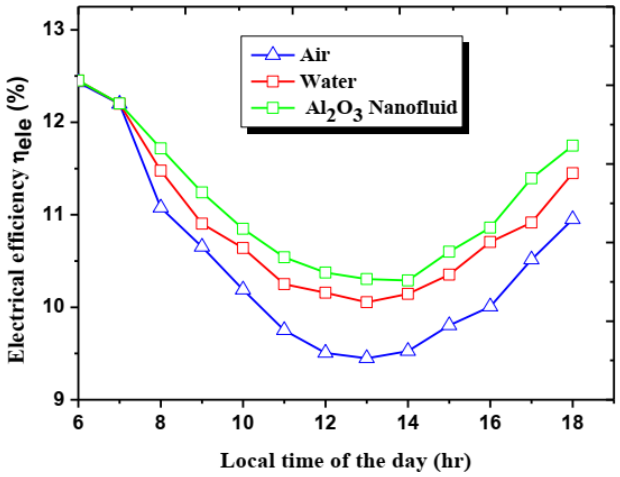

Figure 9. Electrical efficiency variation with the three studied fluids

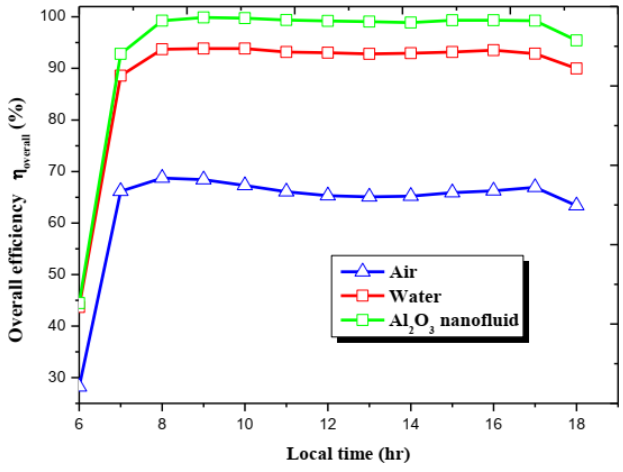

Figure 10. Hourly variation the overall efficiency of the three working fluids

VI. Conclusion

According to the theoretical results obtained from the numerical calculation of the performances of a hybrid photovoltaic/thermal (PV/T) solar collector, using three different cooling fluids: Alumina nanofluid, water and air, the following conclusions have been drawn:

- ✓ The model was validated and the results obtained are in good agreement with those reported by literature.
- ✓ The increase in mass flow rate extending over the range: 0.005-0.04 kg/s, leads to raise the efficiencies by decreasing the heat losses from absorbing plates to the ambiance.
- ✓ The outlet temperature of the system using nanofluid is higher than the two other systems using water and air.
- ✓ The results show that using nanofluid as cooling fluid, the electrical efficiency increases due to the decrease of the temperature of the PV cell.
- ✓ The hybrid (PV/T) system using Alumina nanofluid presents the highest thermal efficiency, compared to the system using water and air as working fluids, respectively (73.28%, 67.67% and 41.55%).
- ✓ The overall efficiency of the system using nanofluid (99.21%) is higher than water (93.06%) and air (65.31%), because the presence of nanoparticles in water increases the thermal proprieties of this fluid.

NOMENCLATURE

A: the area of the component of the system, m^2
c_p : the specific heat of the component of the system, J/kg .K
D_h : hydraulic diameter, m
e: The thickness of the component , m
h_{vg} is the convective heat transfer coefficient between the glazing and ambiance, $W/m^2.K$
h_{rg} is the radiation heat transfer coefficient from the glazing to the sky, $W/m^2.K$
h_{vc} is the convection heat transfer coefficient for air cavity between the solar cell and glazing, $W/m^2.K$
h_{rc} is the radiation heat transfer coefficient between solar cell and glazing, $W/m^2.K$
h_{cc} is the heat transfer coefficient conduction between the PV cell and the absorber plate, $W/m^2.K$
h_{vp} is the heat transfer coefficient convection between the absorber plate and the fluid, $W/m^2.K$
h_{rp} is the heat transfer coefficient by radiation between the absorber and back plate, $W/m^2.K$
h_{vbp} is the heat transfer coefficient convection between the fluid and the back plate, $W/m^2.K$
h_{ci} is the heat transfer conduction coefficient in the insulation, $W/m^2.K$
h_{ra} is the radiation heat transfer coefficient from the back plate and soil, $W/m^2.K$
h_{va} is the convective heat transfer coefficient for air cavity between the back plate and soil, $W/m^2.K$

$Q_{ele}$is the electrical power produced by the PV module, W/m^2
g:the gravitational constant, m^2/s.
k: thermal conductivity W/m.K
m: the mass of the component of the system, kg
$\dot{m}$ is the mass flow rate of the fluid, kg/s
Nu represents the Nusselt number
P: the energy absorbed by the component of the system, W/m^2
P_{dir} and P_{dif} represents respectively the intensity of the direct and diffuse incident radiation, W/m^2
$R_a$represents the Rayleigh number
T: temperature, K, °C
t: time, hr
v the wind velocity, m/s

INDEX
a: ambient
air: air
bp: back plate
c: PV cell
f : fluid
g: Glass
i: insolating
in: inlet
nf: nanofluid
out: outlet
p: absorbing plate.
s: sky
soil: soil
water: water

GREC SYMBOLS
α_{V1-dir} et α_{V1-dif} : the absorption coefficients of glazing
σ is the stephan-Boltzmann constant, $\sigma = 5.67\times10^{-8}$ W·m^{-2}·K^{-4}
s is the emissivity of thermal radiation of the component.
θ : the collector inclination angle, °
ρ : the density, kg/ m^3
β : thermal expansion coefficient, 1/K
β_c is the Packing factor
β_r is the temperature coefficient
μ : the dynamic viscosity
φ : volume fraction of Al_2O_3 nanoparticules
5_{ele} design the electrical efficiency generated by the cell, %
5_{ref} is the reference cell efficiency, %
5_{th}The instantaneous thermal efficiency of the PV/T collector, %
$5_{overall}$ the overall efficiency of the PV/T solar collector, %

References

[1] A. Ibrahim, M.Y. Othman, M.H. Ruslan, S. Mat, K. Sopian. "Recent advances in flat plate photovoltaic/thermal (PV/T) solar collectors", Renewable and Sustainable Energy Reviews, Vol. 15, 2011, pp. 352-365.

[2] F. Hussain, M.Y. H. Othman, K. Sopian, B. Yatim, H. Ruslan, H. Othman. "Design development and performance evaluation of photovoltaic/ thermal (PV/T) air base solar collector", Renewable and Sustainable Energy Reviews, Vol. 25, 2013, pp. 431-441.

[3] J. Prakash. "Transient analysis of a photovoltaic/ thermal solar collector for co-generation of electricity and hot air/water," Energy Conversion and Management, 1994, Vol. 35, pp. 967-972.

[4] K. Sopian, K. S. Yigit, H. T. Liu, S.Kakaç , T.N. Veziroglu. "Performance analysis of photovoltaic thermal air heaters," Energy Conversion and Management, 1996, Vol. 37, pp. 1657-1670.

[5] A. Hegazy. "Comparative study of the performances of four photovoltaic/thermal solar air system," Energy Conversion and Management, 2000, Vol. 41, pp. 861-881.

[6] H.A.Zondag, D.W de Vries , W.G.J.Van .Helden, R.J.C. Van Zolingen, A.A. van Steenhoven. "The yield of different combined PV-Themal collector designs," Solar Energy 2003, Vol. 74, pp. 253-269.

[7] T. T. Chow. "Performance analysis of photovoltaic-thermal collector by explicit dynamic model," Solar Energy, 2003, Vol. 75, pp. 143-152.

[8] J. K. Tonui, Y.Tripanagnostopoulos. "Air-cooled PV/T solar collectors with low cost performance improvements," Solar Energy, 2007, Vol. 81, pp. 498-511.

[9] Y. Tripanagnostopoulos. "Aspects and improvements of hybrid photovoltaic/ thermal solar energy systems", Solar Energy, 2007, Vol. 81, pp. 1117-1131.

[10] E. Shojaeizadeh, F. Veysi, T. Yousefi, F. Davodi. "An experimental investigation on the efficiency of a flat-plate solar collector with binary working fluid: A case study of propylene glycol (PG)-water," Experimental Thermal and Fluid Science, 2014, Vol. 53, pp. 218-226.

[11] C. Cristofari, G. Notton, J. L. Canaletti. "Thermal behavior of a copolymer PV/TH solar system in low flow rate conditions", Solar Energy, 2009, Vol. 83, pp. 1123-1138.

[12] R. Kumar, M. A. Rosen. "Performance evaluation of a double pass PV/T solar air heater with and without fins," Applied Thermal Engineering, 2011, Vol. 31, pp. 1402-1410.

[13] L. A. Tagliafico, F. Scarpa, M. D. Rosa. "Dynamic thermal models and CFD analysis for flat plate thermal solar collectors- A review", Renewable and Sustainable Energy Reviews, 2014, Vol. 30, 526-537.

[14] O. Mahian, A.Kianifar , S.A.Kalogirou, I. Pop, S. Wongwises. "A review of the applications of nanofluids in solar energy," International Journal of Heat and Mass Transfer, 2013, Vol. 57, pp. 582-594.

[15] M. Faizal, R. Saidur, S. Mekhilef, M.A.Alim. "Energy economic and environmental analysis of metal oxides nanofluid for flat plate collector," Energy Conversion and Management, 2013, Vol. 76, pp. 162-168.

[16] J. Sarkar. "A critical review on convective heat transfer correlations of nanofluids," Renewable and Sustainable Energy Reviews, 2011, Vol. 15, pp. 3271-3277.

[17] L. Godson, B. Raja, D. M. Lal, S. Wongwises. "Enhancement of heat transfer using nanofluids- An overview," Renewable and Sustainable Energy Reviews, 2010, Vol. 14, pp. 629-641.

[18] X- Q. Wang, A.S. Mujumdar. "A review on nanofluids-part1: Theoretical and numerical investigations," Brazilian Journal of Chemical Engineering, 2008, Vol. 25, pp. 613-630.

[19] Y. Xuan, Q. Li. "Investigation on convective heat transfer and flow features of nanofluids," Journal of Heat Transfer, 2003, Vol. 125, pp. 151-155.

[20] R.S. Vajjha, D.K. Das. "A review and analysis on influence of temperature and concentration of nanofluids on thermophysical properties, heat transfer and pumping power," International Journal of Heat and Mass Transfer, 2012, Vol. 55, pp. 4063-4078.

[21] R. Kandasamy, I.Muhaimin, A.K.Rosmila. "The performance evaluation of unsteady MHD non-Darcy nanofluid flow over a porous wedge due to renewable (solar) energy," Renewable Energy, 2014, Vol. 64, pp. 1-9.

[22] M. Rostanami, S. F. Hosseinizadeh, M. Gorji, J. M. Khodadadi. "Numerical study of turbulent forced convection flow of nanofluids in a long horizontal duct considering variable properties," International Communications in Heat and Mass Transfer, 2010, Vol. 37, pp. 1426-1431.

[23] T. Yousefi, F. Veysi, E. Shojaeizadeh, S. Zinadini. "An experimental investigation on the effect of Al_2O_3 – H_2O nanofluid on the efficiency of flat plate solar collectors," Renewable Energy, 2012, Vol. 39, pp. 293-298.

[24] R. Saidur, T. C. Meng, Z. Said, M. Hasanuzzaman, A. Kamyar. "Evaluation of the effect of nanofluid-based absorbers on direct solar collector," International Journal of Heat and Mass Transfer, 2012, Vol. 55, pp. 5899-5907.

[25] H. Vishwanadula, E. C. Nsofor. "Studies on forced convection nanofluid flow in circular conduits," ARPN Journal of Engineering and Applied Sciences, 2012, Vol. 7, pp. 371-376.

[26] Z. Said, M.H.Sajid, M.A.Alim, R.Saidur, N.A.Rahim. "Experimental investigation of the thermophysical proprieties of AL2O3- nanofluid and its effect on a flat plate solar collector," International Communications in Heat and Mass Transfer, 2013, Vol. 48, pp. 99-107.

[27] S. E. B. Maiga, S. J. Palm, C. T. Nguyen, G. Roy, N. Galanis. "Heat transfer enhancement by using nanofluids in forced convection flows," International Journal of Heat and Fluid Flow, 2005, Vol. 26, pp. 530-546.

[28] J. A. Duffie, W. A. Beckman. "Solar Engineering of Thermal Processes," John Wiley & Sons Inc, New York, 1991.

[29] K. S. Ong. "Thermal performance of solar air heaters: Mathematical model and solution procedure," Solar Energy, 1995, Vol. 55, pp. 93-109.

[30] G. N. Tiwari and Swapnil Dubey. "Fundamentals of Photovoltaic Modules and Their Applications," RSC Energy Series N° 2, 2010.

[31] Incropera, DeWitt, Bergman, Lavine. "Fundamentals of Heat and Mass Transfer", Johns Wiley & Sons, 2006.

[32] A. I. Kudish, E. G. Evseev, G. Walter, T. Leukefeld. "Simulation study of a solar collector with a selectively coated polymeric double walled absorber plate," Energy Conversion and Management, 2002, Vol. 43, pp. 651-671.

[33] S. E. B. Maiga, C. T. Nguyen, N. Galanis, G. Roy. Heat transfer behaviours of nanofluids in a uniformly heated tube," Super Lattices and Microstructures, 2004, Vol. 35, pp. 543-557.

[34] J.S. Jayakumar, S.M. Mahajania, J.C. Mandala, Kannan N. Iyer, P.K. Vijayan. "CFD analysis of single-phase flows inside helically coiled tubes", Computers and Chemical Engineering, 2010, Vol. 34, pp. 430–446.

[35] E. Abu-Nada. "Effects of variable viscosity and thermal conductivity of Al_2O_3-water nanofluid on heat transfer enhancement in natural convection," International Journal of Heat and Fluid Flow, 2009, Vol. 30, pp. 679-690.

[36] J.P. Holman. "Heat Transfer," MC Graw-Hill series in Mechanical Engineering, 2010. 10th edition.

[37] http://www.accuweather.com/fr/dz/constantine/ 10/01/22021